Tim Osswald

Understanding Polymer Processing

Processes and Governing Equations

Sample Chapter 2:
Mechanical Behavior of Polymers

ISBNs
978-1-56990-472-5
1-56990-472-3

HANSER
Hanser Publishers, Munich • Hanser Publications, Cincinnati

2 Mechanical Behavior of Polymers

The mechanical properties of a polymeric component are dominated by its viscoelasticity. This is reflected by the time-dependency of the mechanical response of a component during loading. Hence, a polymer behaves differently if subjected to short term or long term loads. This chapter briefly explains polymer viscoelasticity and covers the short and long term mechanical behavior of polymers.

2.1 Viscoelastic Behavior of Polymers

A polymer, at a specific temperature and molecular weight, may behave as a liquid or a solid, depending on the speed (time scale) at which its molecules deform. This behavior, which ranges between liquid and solid, is generally referred to as the viscoelastic behavior or material response. This discussion is limited to *linear viscoelasticity*, which is valid for polymer systems undergoing *small or slow deformations*. *Non-linear viscoelasticity* is required when modeling *large rapid deformations,* such as those encountered in flowing polymer melts.

In linear viscoelasticity, the *stress relaxation test* is often used, along with the *time-temperature superposition principle* and the *Boltzmann superposition principle*, to explain the behavior of polymeric materials during deformation.

2.1.1 Stress Relaxation

In a stress relaxation test, a polymer specimen is suddenly deformed by a fixed amount, ϵ_0, and the stress required to hold that amount of deformation is recorded over time. This test is cumbersome to perform, so the design engineer and the material scientist have tended to ignore it. In fact, the standard relaxation test, ASTM D2991, was dropped by ASTM in the early 1990s. Rheologists and scientists, however, have consistently used the stress relaxation test to interpret the viscoelastic behavior of polymers.

Figure 2.1 [1] presents the stress relaxation modulus measured for polyisobutylene[1)] at various temperatures. Here, the stress relaxation modulus is defined by

$$E_r = \frac{\sigma(t)}{\varepsilon_0} \tag{2.1}$$

where ε_0 is the applied strain and $\sigma(t)$ the stress being measured. From the test results, stress relaxation is clearly time and temperature dependent, especially around the glass transition temperature where the curve is steepest. For the polyisobutylene in Fig. 2.1, the glass transition temperature is about –70 °C. The measurements were completed in

1) Better known as the matrix material for chewing gum.

an experimental time window between a few seconds and one day. The tests performed at lower temperatures were used to record the initial relaxation while the ones at higher temperatures only captured the end of relaxation of the rapidly decaying stresses. The tests at various temperatures can be used to assemble a master curve at one of the test temperatures, as is shown for 25 °C on the right side of Fig. 2.1.

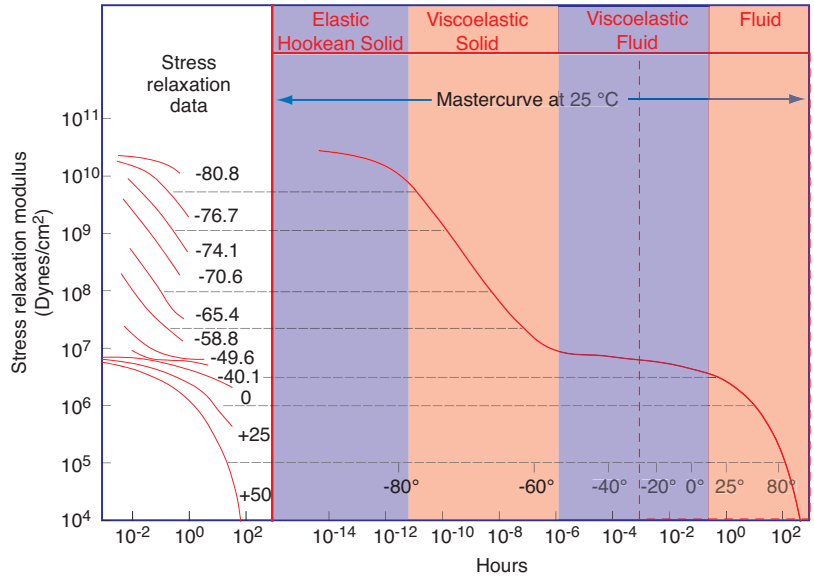

Figure 2.1 Relaxation modulus curves for polyisobutylene and corresponding master curve at 25 °C

The time it takes for the imposed stresses to relax is governed by the relaxation time, λ. For the 25 °C case, the relaxation time is about 100 hours. High temperatures lead to small molecular relaxation times and low temperatures lead to materials with long relaxation times. When changing temperature, the shape of relaxation test results remains the same, except for a horizontal shift to the left or right, representing lower or higher response times, respectively.

2.1.2 Time-Temperature Superposition

The time-temperature equivalence seen in stress relaxation test results can be used to reduce data at various temperatures to one general *master curve* for a reference temperature, T. To generate a master curve at any reference temperature, the curves shown on the left of Fig. 2.1 must be shifted horizontally, holding the reference curve fixed. The master curve for the data in Fig. 2.1 is on the right of the figure. Each curve was shifted horizontally until the ends of all the curves superposed. The amount that each curve was shifted can be plotted with respect to the temperature difference taken from the reference temperature. For the data in Fig. 2.1, the shift factor is shown in

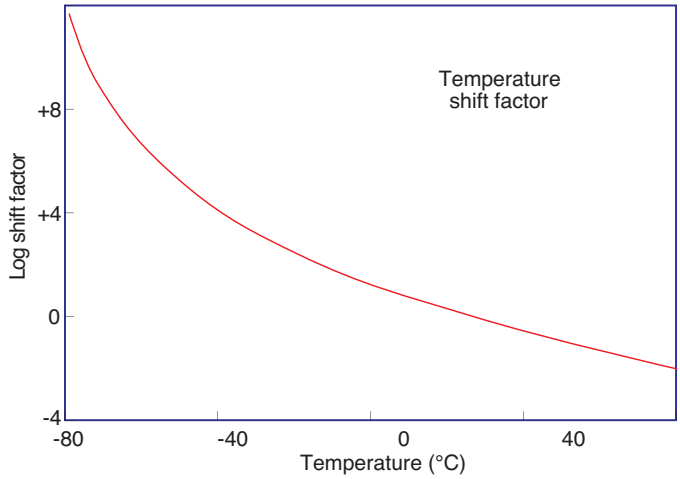

Figure 2.2 Shift factor as a function of temperature used to generate the master curve plotted in Fig. 2.1

Fig. 2.2. It is important to point out here that the relaxation master curve represents a material at a single temperature, but depending on the time scale, it can be regarded as a Hookean solid, or a viscous fluid. In other words, if the material is loaded for a short time, the molecules are not allowed to move and slide past each other, resulting in a perfectly elastic material. In such a case, the deformation is fully recovered. However, if the test specimen is maintained deformed for an extended period of time, such as 100 hours for the 25 °C case, the molecules will have enough time to slide and move past each other, fully relaxing the initial stresses, resulting in permanent deformation. For such a time scale the material can be regarded as a fluid.

WLF Equation [2]

The amount relaxation curves must be shifted in the time axis to line-up with the master curve at a reference temperature is represented by

$$\log t - \log t_{\text{ref}} = \log\left(\frac{t}{t_{\text{ref}}}\right) = \log a_T \tag{2.2}$$

Although the results in Fig. 2.2 where shifted to a reference temperature of 298 K (25 °C), Williams, Landel and Ferry [2] chose $T_{\text{ref}} = 243$ K for

$$\log a_T = \frac{-8.86\,(T - T_{\text{ref}})}{101.6 + T - T_{\text{ref}}} \tag{2.3}$$

which holds for nearly all amorphous polymers if the chosen reference temperature is 45 K above the glass transition temperature. In general, the horizontal shift, $\log a_T$,

between the relaxation responses at various temperatures to a reference temperature can be computed using the well known Williams-Landel-Ferry [2] (WLF) equation. The WLF equation is

$$\log a_T = \frac{-C_1(T - T_{\text{ref}})}{C_2 + T - T_{\text{ref}}} \tag{2.4}$$

where C_1 and C_2 are material dependent constants. It has been shown that with $C_1 = 17.44$ and $C_2 = 51.6$, Eq. 2.4 fits well for a wide variety of polymers as long as the glass transition temperature is chosen as the reference temperature. These values for C_1 and C_2 are often referred to as universal constants. Often, the WLF equation must be adjusted until it fits the experimental data. Master curves of stress relaxation tests are important because the polymer's behavior can be traced over much longer periods than those that can be determined experimentally.

Boltzmann Superposition Principle

In addition to the *time-temperature superposition principle* (WLF), the *Boltzmann superposition principle* is of extreme importance in the theory of linear viscoelasticity. The Boltzmann superposition principle states that the deformation of a polymer component is the sum or superposition of all strains that result from various loads acting on the part at different times. This means that the response of a material to a specific load is independent of pre-existing loads. Hence, we can compute the deformation of a polymer specimen upon which several loads act at different points in time by simply adding all strain responses.

2.2 The Short-Term Tensile Test

The most commonly used mechanical test is the short-term stress-strain tensile test. Stress-strain curves for selected polymers are displayed in Fig. 2.3 [3]. For comparison, the figure also presents stress-strain curves for copper and steel. Although they have much lower tensile strengths, many engineering polymers exhibit much higher strains at break than metals.

The next two sections discuss the short-term tensile test for cross-linked elastomers and thermoplastic polymers separately. The main reason for separating these two polymers is that the deformation of a crosslinked elastomer and an uncrosslinked thermoplastic differ greatly. The deformation in a crosslinked polymer is generally reversible, while the deformation in typical uncross-linked polymers is associated with molecular chain relaxation, making the process time-dependent and irreversible.

2.2.1 Elastomers

The main feature of cross-linked elastomeric materials is that they can undergo large, reversible deformations. This is because the curled polymer chains stretch during

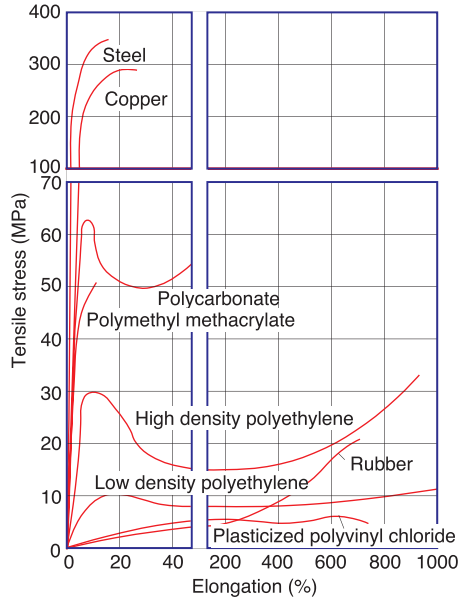

Figure 2.3 Tensile stress-strain curves for several materials

deformation but are hindered from sliding past each other by the crosslinks between the molecules. Once a load is released, most molecules recoil. As an elastomeric polymer component is deformed, the slope in the stress-strain curves drops significantly because the uncurled molecules provide less resistance and entanglement, allowing them to move more freely. Eventually, at deformations of about 400 %, the slope starts to increase because the polymer chains are fully stretched. This stretch is followed by polymer chain breakage or crystallization, ending with the fracture of the component. Stress-deformation curves for natural rubber (NR) [4] and a rubber compound [5] composed of 70 parts of styrene-butadiene-rubber (SBR) and 30 parts of natural rubber are shown in Fig. 2.4.

Because of the large deformations, typically several hundred percent, the stress-strain data is usually expressed in terms of the extension ratio, λ, defined by

$$\lambda = \frac{l}{l_0} \tag{2.5}$$

where l and l_0 are the instantaneous and initial lengths of the specimen, respectively.

For a component in uniaxial extension, or compression, the stress can be computed as

$$\sigma = G_0 \left(\lambda - \frac{1}{\lambda^2} \right) \tag{2.6}$$

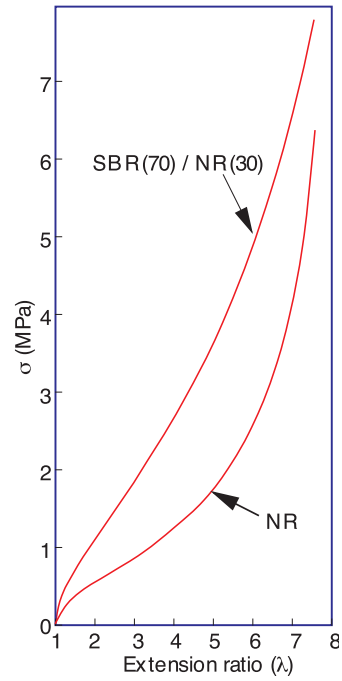

Figure 2.4 Experimental stress-extension curves for NR and a SBR/NR compound

where G_0 is the shear modulus at zero extension, which for rubbers can be approximated by

$$G_0 = \frac{E_0}{3} \tag{2.7}$$

with E_0 as the elastic tensile modulus at zero extension. The model agrees with experiments up to about 50 % extension ($\lambda = 1.5$). For compression, the model agrees much better with experiments, as shown for natural rubber in Fig. 2.5 [4]. Fortunately, rubber products are rarely deformed more than 25 % in compression or tension, allowing the use of the above model.

The corresponding model for equibiaxial extension (inflation) of thin sheets is:

$$\sigma = G_0 \left(\lambda^2 - \frac{1}{\lambda^4} \right) \tag{2.8}$$

2.2.2 Thermoplastic Polymers

Of all the mechanical tests done on thermoplastic polymers, the tensile test is the least understood, and the results are often misinterpreted and misused. Because the test was

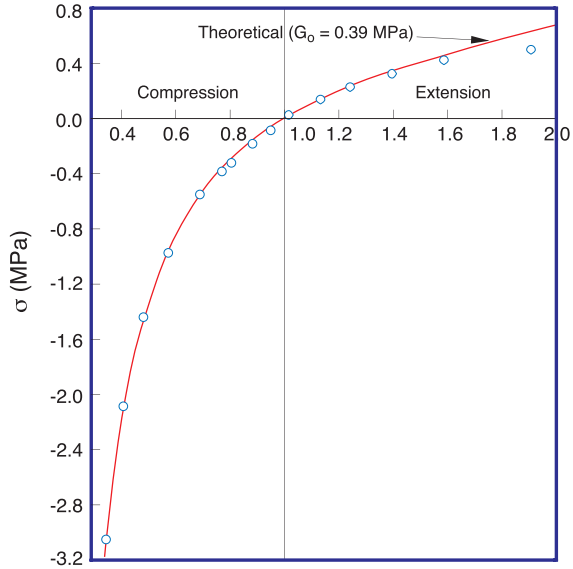

Figure 2.5 Experimental and theoretical stress-extension and compression curves for natural rubber

inherited from other materials that have linear elastic stress-strain responses, it is often inappropriate for testing polymers.

A typical test performed on PMMA at various strain rates at room temperature is shown in Fig. 2.6. The increased curvature in the results with slow elongational speeds suggests that stress relaxation plays a significant role during the test. Here, the high rates of deformation reduce the loading time, allowing higher stress to build-up during the test.

The standard test used to measure the stress-strain behavior of thermoplastic polymers is the widely accepted ASTM D638 test and its ISO counterpart the ISO 527 test. Because the standard test uses a single deformation speed, the resulting moduli, maximum strain and ultimate stress, can only be used when comparing one material against another, and not for design purposes.

The stiffness and strength of polymers and rubbers is increased by filling them with solid particles, such as calcium carbonate and carbon black. The most common expression for describing the effect of carbon black content on the modulus of rubber was originally derived by Guth and Simha [6, 7] for the viscosity of particle suspensions, and later used by Guth to predict the modulus of filled polymers. The Guth equation can be written as

$$\frac{G_f}{G_0} = 1 + 2.5\varphi + 14.1\varphi^2 \tag{2.9}$$

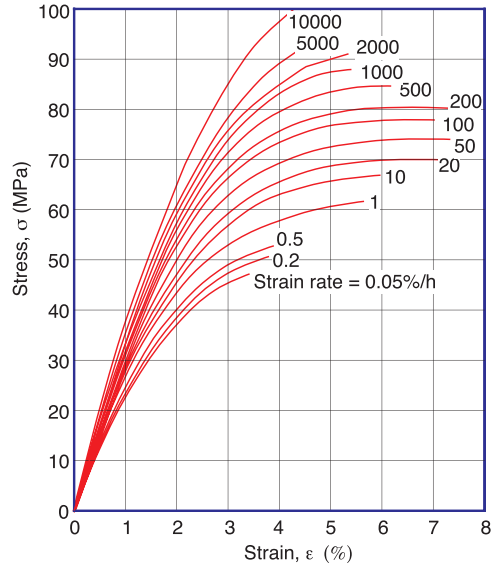

Figure 2.6 Stress-strain behavior of PMMA at various strain rates

where G_f is the shear modulus of the filled material and φ is the volume fraction of particulate filler. The above expression is compared to experiments [8, 9] in Fig. 2.7.

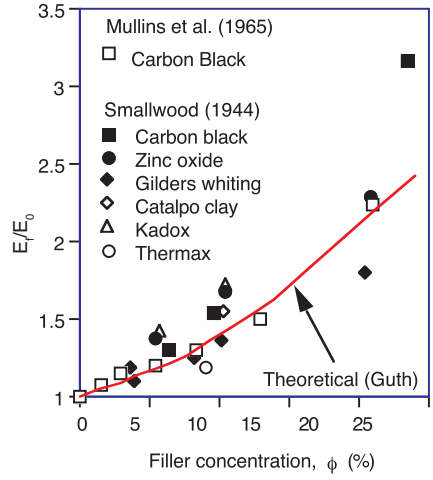

Figure 2.7 Modulus ratio of filled to unfilled natural rubber

2.3 Long-Term Tests

The *stress relaxation* and the *creep* test are well-known long-term tests. The stress relaxation test is difficult to perform and is, therefore, often approximated by data acquired through the more commonly used creep test. The stress relaxation of a polymer is often considered the inverse of creep.

The creep test, which can be performed either in shear, compression, or tension, measures the flow of a polymer component under a constant load. It is a common test that measures the strain, ε, as a function of stress, time, and temperature. Standard creep tests such as DIN 53 444 and ASTM D2990 can be used. Creep tests are performed at a constant temperature, using a range of applied stress, as shown in Fig. 2.8 [10], where the creep responses of a polypropylene copolymer are presented for a range of stresses in a graph with a log-scale for time. If plotting creep data in a log-log graph, in the majority of the cases, the creep curves reduce to straight lines. Hence, the creep behavior of most polymers can be approximated with a power law:

$$\varepsilon(t) = k(T)\,\sigma^m\,t^n \tag{2.10}$$

where $k(T)$, m and n are material dependent properties.

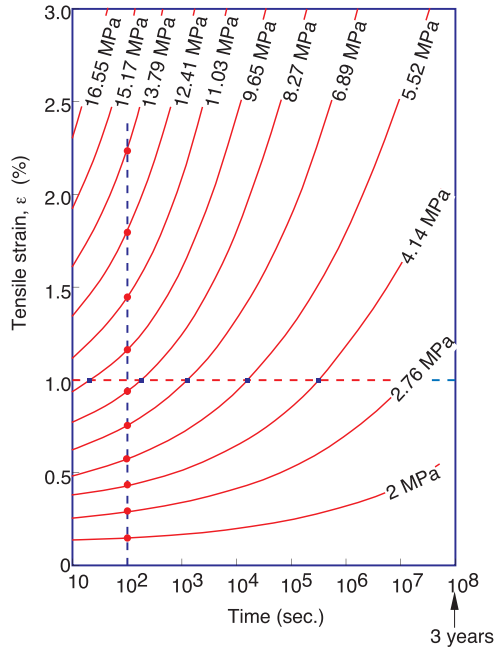

Figure 2.8 Creep response of a propylene-ethylene copolymer at 20 °C

As for the stress relaxation test, the creep behavior of a polymer depends heavily on the material temperature during testing, with the highest rates of deformation near the glass transition temperature.

Creep data is often presented in terms of the creep modulus, E_c, defined by

$$E_c = \frac{\sigma_0}{\varepsilon(t)} \tag{2.11}$$

2.3.1 Isochronous and Isometric Creep Plots

Typical creep test data, shown in Fig. 2.8, can be manipulated to be displayed as short-term stress-strain tests or as stress relaxation tests. These manipulated creep curves are called *isochronous* and *isometric* graphs.

An isochronous plot of the creep data is generated by cutting sections through the creep curves at constant times and plotting the stress as a function of strain, as shown in Fig. 2.8. The isochronous curves of the creep data in Fig. 2.8 are shown in Fig. 2.9 [10, 11]. Similar curves can also be generated by performing a series of *short creep tests*, where a specimen is loaded at a specific stress for a short period, typically around 100 seconds. The load is then removed, and the specimen relaxes for a period of at least four times the loading interval. The specimen is then reloaded at a different stress, and the test is repeated until there are sufficient points for an isochronous graph. This procedure is more expedient than the regular creep test and is often used to predict the short-term behavior of polymers. However, it should be pointed out that the short-term tests described in Section 2.2.2 are more accurate, quicker, and less expensive to run.

The isometric or "equal size" plots of the creep data are generated by taking constant strain sections of the creep curves and by plotting stress versus time. Isometric curves of the polypropylene creep data in Fig. 2.8 are shown in Fig. 2.10 [10]. This plot resembles the stress relaxation test results and is often used similarly. When we divide the stress axis by the strain, we can also plot modulus versus time.

2.3.2 Creep Rupture

A creeping polymer component eventually undergoes catastrophic failure, generally called creep rupture or static fatigue. The standard test for creep rupture is the same as the creep test discussed earlier. Results from creep rupture tests are usually graphs of applied stress versus the logarithm of time to rupture. An example of a creep rupture test that ran for several decades, starting in 1958, is shown in Fig. 2.11 [12, 13]. Here, the creep rupture of HDPE pipes under internal pressures was tested at different temperatures. Two general regions with different slopes become obvious in the plots. The curves to the left of the knee correspond to ductile failure, whereas those to the right correspond to brittle failure. Generating a graph such as the one presented in Fig. 2.11

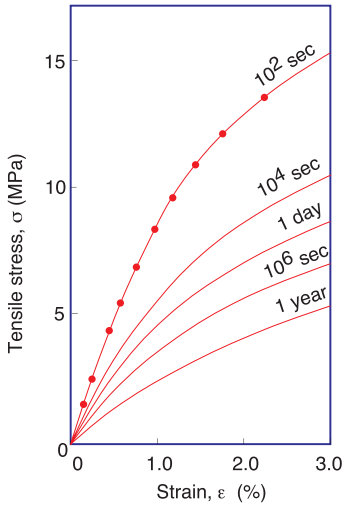

Figure 2.9 Isochronous stress-strain curves for the creep responses in Fig. 2.8

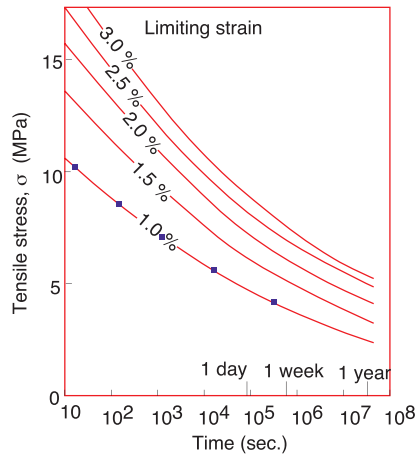

Figure 2.10 Isometric stress-time curves for the creep responses in Fig. 2.8

is lengthy, taking several years of testing. Once the steeper slope, typical of brittle fracture, has been reached, extrapolation with some confidence can be used to estimate future creep rupture times.

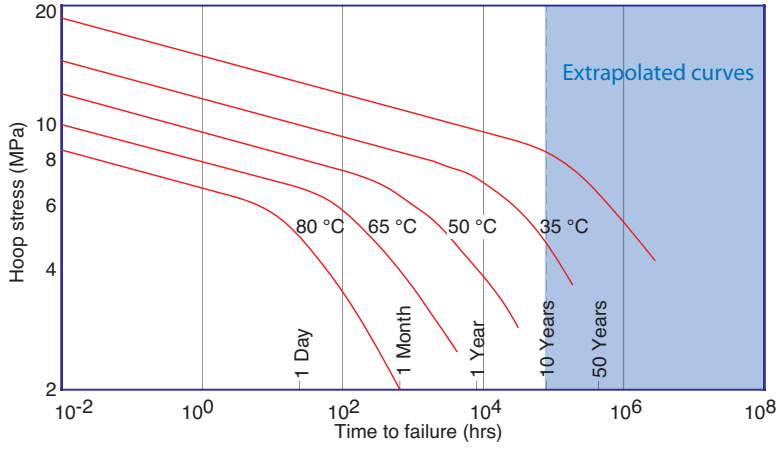

Figure 2.11 Creep rupture behavior as a function of temperature for a HDPE

2.4 Dynamic Mechanical Tests

The sinusoidal oscillatory test, also called the dynamic-mechanical-analysis (DMA) test, is one of the most useful mechanical tests for polymers. Here, a specimen is excited with a low frequency stress input, which is recorded along with the strain response. The shapes of the test specimen and the testing procedure vary significantly from test to test. The various tests and their corresponding specimen shapes are described by ASTM D4065 and the terminology is described by ASTM D4092. The typical responses measured in these dynamic tests are a storage modulus, G', and a loss modulus, G''. The storage modulus is related to the elastic modulus of the polymer at the loading frequency and the loss modulus to the damping or dissipative component observed during loading. The loss modulus can also be written in terms of loss tangent (tan δ) or logarithmic decrement, Δ. The latter is related to the damping of a freely oscillating specimen.

Figure 2.12 [3] shows the elastic shear modulus and the logarithmic decrement or loss factor for various polypropylene grades. Here, the glass transition temperatures and the melting temperatures can be seen for the various polypropylene grades. The vertical scale in plots such as in Fig. 2.12 is usually logarithmic. However, a linear scale better describes the mechanical behavior of polymers in design aspects. Figure 2.13 [3] presents the elastic shear modulus versus temperature on a linear scale for several thermoplastic polymers.

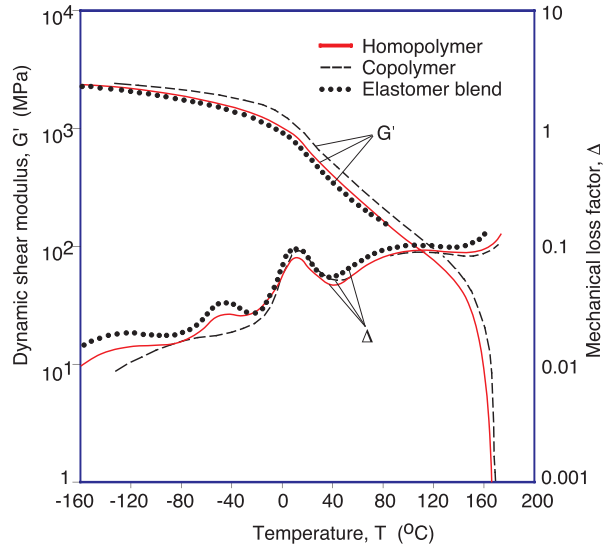

Figure 2.12 Elastic shear modulus and loss tangent for various polypropylene grades

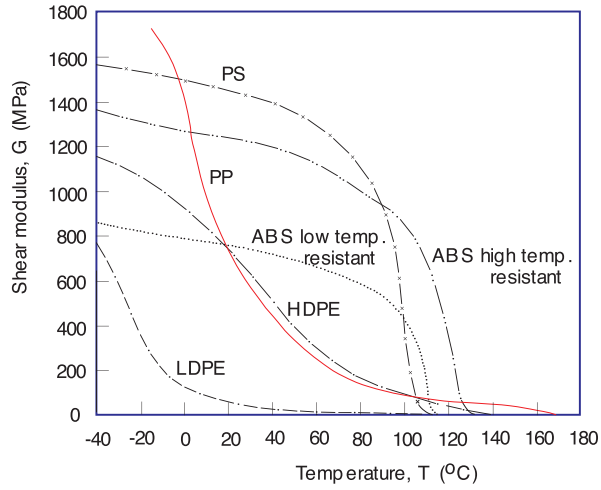

Figure 2.13 Elastic shear modulus for various polymers

If the test specimen in a sinusoidal oscillatory test is linearly elastic, the strain input and stress response would be in phase

$$\gamma = \gamma_0 \sin(\omega t) \tag{2.12}$$

$$\tau = \tau_0 \sin(\omega t) \tag{2.13}$$

For an ideally viscous test specimen (Newtonian), the stress response lags $\frac{\pi}{2}$ radians behind the strain input

$$\gamma = \gamma_0 \sin(\omega t) \tag{2.14}$$

$$\tau = \tau_0 \sin\left(\omega t - \frac{\pi}{2}\right) \tag{2.15}$$

Polymers behave somewhere in between these cases and their response is described by

$$\gamma = \gamma_0 \sin(\omega t) \text{ and} \tag{2.16}$$

$$\tau = \tau_0 \sin(\omega t - \delta) \tag{2.17}$$

which results in a complex shear modulus

$$G^* = \frac{\tau(t)}{\gamma(t)} = \frac{\tau_0 e^{i\delta}}{\gamma_0} = \frac{\tau_0}{\gamma_0}(\cos\delta + i\sin\delta) = G' + G'' \tag{2.18}$$

where G' is usually called the *storage modulus* and G'' is the *loss modulus*. The ratio of loss modulus to storage modulus is called the *loss tangent:*

$$\tan\delta = \frac{G''}{G'} \tag{2.19}$$

Although the elastic shear modulus, G' and the loss modulus G'', are sufficient to characterize a material, one can also compute the logarithmic decrement, Δ, or loss factor by using

$$\Delta = \frac{G''\pi}{G'} \tag{2.20}$$

The logarithmic decrement can also be written in terms of *loss tangent,* $\tan\delta$, where δ is the mechanical loss angle. The loss tangent is then

$$\tan\delta = \frac{G''}{G'} = \frac{\Delta}{\pi} \tag{2.21}$$

2.5 Mechanical Behavior of Filled and Reinforced Polymers

Fillers are materials intentionally inserted in polymers to make them stronger, lighter, electrically conductive, or less expensive. Any filler affects the mechanical behavior of a polymeric material. For example, long fibers make the polymer stiffer but usually denser, whereas foaming makes it more compliant and much lighter. On the other hand, a filler, such as calcium carbonate, decreases the polymer's toughness, while making it considerably cheaper to produce.

Reinforced plastics are matrix polymers whose properties have been enhanced by introducing a reinforcement (fibers) of higher stiffness and strength. Such a material is usually called a *fiber reinforced polymer* (FRP) or a *fiber reinforced composite* (FRC). The purpose of introducing a fiber into a matrix is to transfer the load from the weaker material to the stronger one. This load transfer occurs over the length of the fiber as shown in Fig. 2.14.

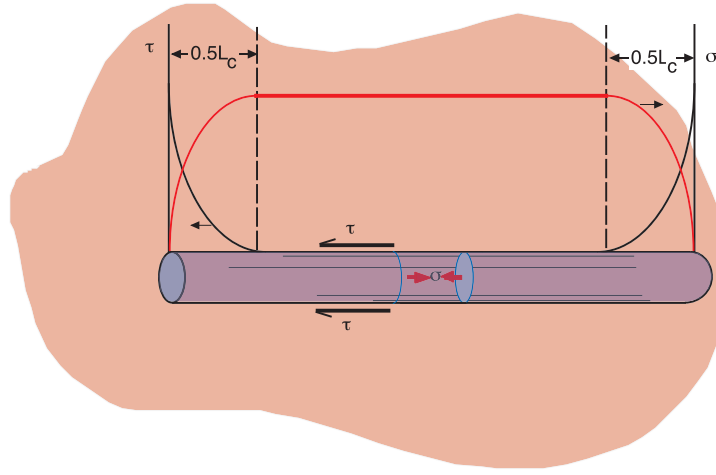

Figure 2.14 Schematic diagram of load transfer from matrix to fiber in a composite

The length to complete the load transfer from the matrix to the fiber, without fiber or matrix fracture, is usually called the critical length, L_c. For the specific case, where there is perfect adhesion between fiber and matrix, experimental evidence suggests that aspect ratios of 100 or higher are required for maximum strength [14]. If composites have fibers that are shorter than their critical length, they are referred to as *short fiber composites*. If the fibers are longer, they are called *long fiber composites* [15].

Halpin and Tsai [16] developed a widely used model to predict the mechanical properties of aligned fiber reinforced composite laminates. With the notation in Fig. 2.15, where f and m represent the fiber and matrix, respectively; L the fiber length; D the fiber diameter; φ the volume fiber fraction, the longitudinal (L) and transverse (T) properties can be predicted using

$$E_L = E_m \left(\frac{1 + \xi \eta \varphi}{1 - \eta \varphi} \right) \tag{2.22}$$

$$E_T = E_m \left(\frac{1 + \eta\varphi}{1 - \eta\varphi} \right) \tag{2.23}$$

$$G_{LT} = G_m \left(\frac{1 + \lambda\varphi}{1 - \lambda\varphi} \right) = G_m \frac{\nu_{LT}}{\nu_m} \tag{2.24}$$

where,

$$\eta = \frac{\left(\frac{E_f}{E_m} - 1 \right)}{\left(\frac{E_f}{E_m} + \xi \right)} \tag{2.25}$$

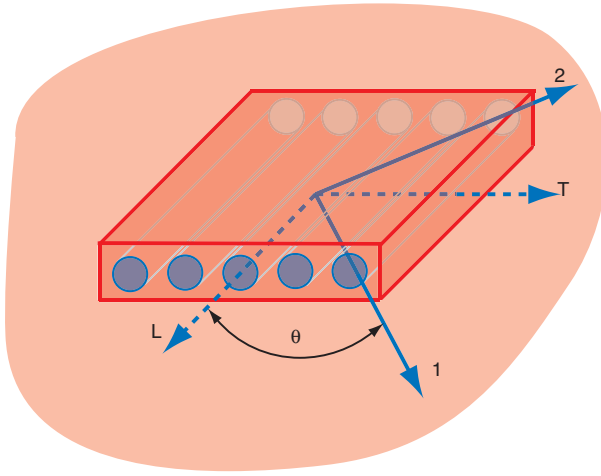

Figure 2.15 Schematic diagram of unidirectional, continuous fiber reinforced laminated structure

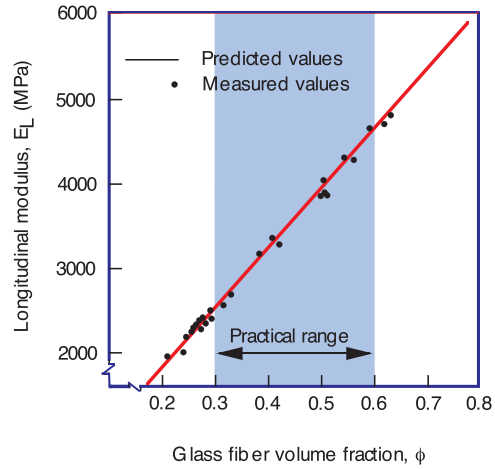

Figure 2.16 Measured and predicted longitudinal modulus for an unsaturated polyester/aligned glass fiber composite laminate as a function of volume fraction of glass content

$$\lambda = \frac{\left(\frac{G_f}{G_m} - 1\right)}{\left(\frac{G_f}{G_m} + 1\right)} \tag{2.26}$$

$$\xi = 2\frac{L}{D} \tag{2.27}$$

Most models accurately predict the longitudinal modulus, as shown in Fig. 2.16 [17]. However, differences do exist between models when predicting the transverse modulus, as shown in Fig. 2.17 [17].

Figure 2.18 [18] shows how the stiffness decreases as one rotates away from the longitudinal axis for an aligned fiber reinforced composite with different volume fraction fiber content.

For high volume fraction fiber contents, only a slight misalignment of the fibers from the loading direction results in drastic property reductions.

The stiffness in a long fiber reinforced composite with a random planar orientation, such as encountered in sheet molding compound (SMC) charges, can be estimated using

$$E_{11} = E_{22} = E_{\text{random}} = \left(\frac{3}{8}\frac{1}{E_L} + \frac{3}{8}\frac{1}{E_T} - \frac{2}{8}\frac{\nu_{LT}}{E_L} + \frac{1}{8}\frac{1}{G_{LT}}\right)^{-1} \tag{2.28}$$

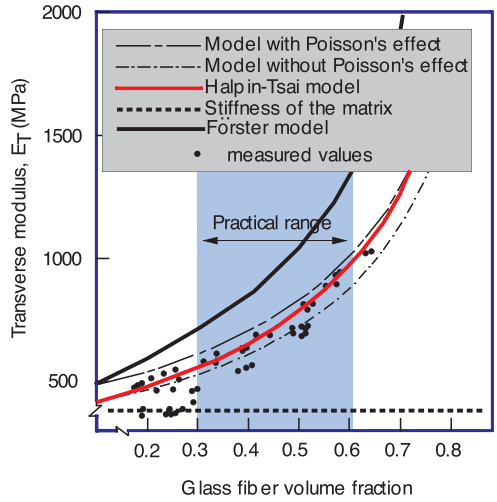

Figure 2.17 Measured and predicted transverse modulus for an unsaturated polyester/aligned glass fiber composite laminate as a function of volume fraction of glass content

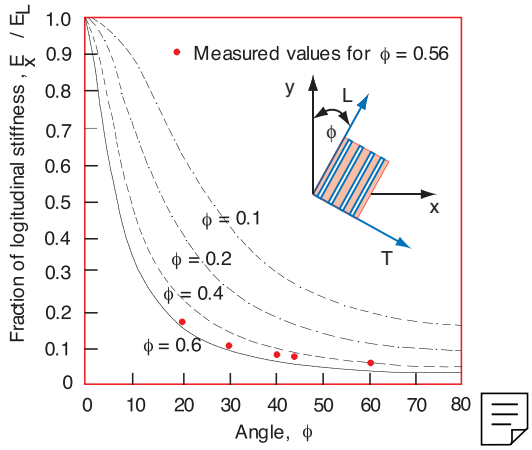

Figure 2.18 Measured and predicted elastic modulus in a unidirectional fiber reinforced laminate as a function of angle between loading and fiber direction

2.6 Impact Strength

In practice, nearly all polymer components are subjected to impact loads. Since many polymers are tough and ductile, they are often well suited for this type of loading. However, under specific conditions even the most ductile materials, such as polypropy-

Table 2.1 Minimum Elongation at Break under Impact Loading

Polymer	ε_{min} (%)
HMW-PMMA	2.2
PA6 + 25 % SFR	1.8
PP	1.8
uPVC	2.0
POM	4.0
PC + 20 % SFR	4.0
PC	6.0

Table 2.2 Minimum Stress at Break on Impact Loading

Polymer	σ_{min} (MPa)
HMW-PMMA	135
PA6 + 25 % Short fiber reinforced (SFR)	175
uPVC	125
POM	> 130
PC + 20 % SFR	> 110
PC	> 70

lene, can fail in a brittle manner at low strains. These types of failure are prone to occur at low temperatures during high deformation rates.

According to several researchers [19, 20], a significantly high rate of deformation leads to complete embrittlement of polymers, resulting in a lower threshold of elongation at break. Menges and Boden designed a special high-speed elongational testing device to measure the minimum work required to break specimens. The minimum strain, ϵ_{min}, which can be measured with such a device, is a safe value to use in design calculations. One should always assume that if this minimum strain is exceeded anywhere in the component, initial fracture has already occurred. Table 2.1 [21] presents minimum elongation at break values for selected thermoplastics under impact loading.

On the other hand, the stiffness and the stress at break of the material under consideration increases with the rate of deformation. Table 2.2 [21] presents data for the stress at break, σ_{min}, for selected thermoplastics under impact loading. This stress corresponds to the point where the minimum elongation at break has just been reached.

Figure 2.19 summarizes the stress-strain and fracture behavior of a HMW-PMMA tested at various rates of deformation. The area under the stress-strain curves represents the *volume-specific energy to fracture* (w). For impact, the elongation at break of 2.2 % and the stress at break of 135 MPa represent a minimum of volume-specific energy, because the stress increases with higher rates of deformation, but the elongation at break remains constant. Hence, if we assume a linear behavior, the *minimum*

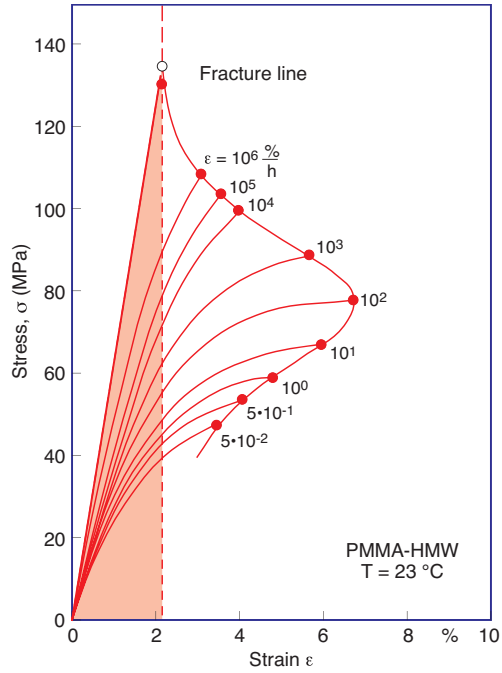

Figure 2.19 Stress-strain behavior of HMW-PMMA at various rates of deformation

volume-specific energy absorption to fracture can be calculated using

$$w_{\min} = \frac{1}{2}\sigma_{\min}\varepsilon_{\min} \tag{2.29}$$

If the stress-strain distribution in the polymer component is known, one can estimate the minimum energy absorption capacity using $w_{\min}$. It can be assumed that failure occurs if $w_{\min}$ is exceeded anywhere in the loaded component. This minimum volume-specific energy absorption, $w_{\min}$, can be used as a design parameter. It can also be used for fiber reinforced polymeric materials [22].

2.7 Fatigue

Dynamic loading of any material that leads to failure after a certain number of cycles is called *fatigue* or *dynamic fatigue*. Dynamic fatigue is of extreme importance because a cyclic or fluctuating load causes a component to fail at much lower stresses than it does under monotonic loads [23]. Dynamic fatigue is of extreme importance since a cyclic or fluctuating load causes a component to fail at much lower stresses than it does under monotonic loads.

Fatigue test results are plotted as stress amplitude versus number of cycles to failure. These graphs are usually called *S-N curves*, a term inherited from metal fatigue testing.

Figure 2.20 [24] presents S-N curves for several thermoplastic and thermoset polymers tested at a frequency of 30 Hz and about a zero mean stress, σ_m.

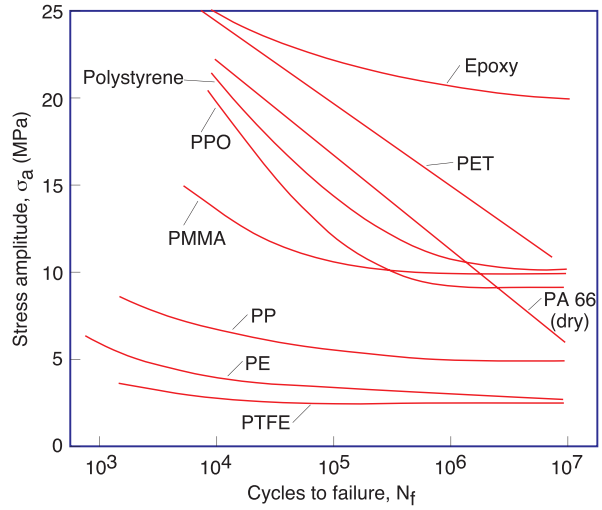

Figure 2.20 Stress-life (S-N) curves for several thermoplastic and thermoset polymers tested at a 30 Hz frequency about a zero mean stress

Fatigue in plastics is strongly dependent on the environment, the temperature, the frequency of loading, and surface finish. For example, because of surface irregularities and scratches, crack initiation at the surface is more likely in a polymer component that has been machined than in one that was injection molded. An injection molded article is formed by several layers of different orientation. In such parts, the outer layers act as a protective skin that inhibits crack initiation. In an injection molded part, cracks are more likely to initiate inside the component by defects such as weld lines and filler particles. The gate region is also a prime initiator of fatigue cracks. Corrosive environments also accelerate crack initiation and failure via fatigue.

Temperature increases during testing is one of the main causes of failure when experimentally testing thermoplastic polymers under cyclic loads. The temperature rise during testing is caused by the combination of internal frictional or hysteretic heating and low thermal conductivity. At low frequency and stress, the temperature in the polymer specimen will rise and can eventually reach thermal equilibrium when the heat generated by hysteretic heating equals the heat removed from the specimen by conduction. As the frequency is increased, viscous heat is generated faster, causing the temperature to rise even further. After thermal equilibrium has been reached, a specimen eventually fails by conventional brittle fatigue, assuming the stress is above the endurance limit. However, if the frequency or stress level is increased even further, the temperature rises to the point that the test specimen softens and ruptures before reaching thermal equilibrium. This mode of failure is usually referred to as *thermal fatigue.*

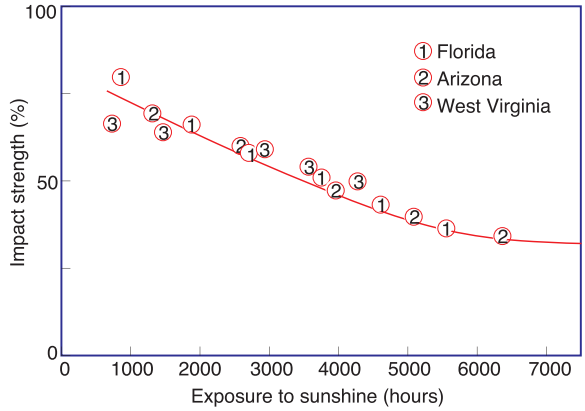

Figure 2.21 Impact strength of an ABS as a function of hours of actual sunlight exposure

2.8 Weathering

When exposed to the elements, polymeric materials can exhibit environmental cracks, which lead to failure at stress levels significantly lower than the ones determined under specific lab conditions. Ultraviolet radiation, moisture, and extreme temperatures harm the mechanical properties of plastic parts.

The strength losses and discoloration from weathering are mainly attributed to the ultra-violet rays in sunlight. This can be demonstrated by plotting properties as a function of sunlight exposure instead of total time exposed. Figure 2.21 [25] is a plot of percent of initial impact strength for an ABS as a function of sunlight exposure in three different locations: Florida, Arizona, and West Virginia. The curve reveals that by "normalizing" the curves with respect to exposure to sunshine, the three different sites with three completely different weather conditions lead to the same relationship between impact strength and sunlight exposure.

The effect of weathering can often be mitigated with pigments, such as TiO_2 or carbon black, which absorb ultraviolet radiation, preventing penetration through the polymer component surface.

Example 2.1 Stress Relaxation

For the poly-α-methylstyrene stress relaxation data in Fig. 2.22 [26], create a master creep curve at T_g (204 °C). Identify the glassy, rubbery, viscous, and viscoelastic regions of the master curve. Identify each region with a spring-dashpot model diagram.

The master creep curve for the above data is generated by sliding the individual relaxation curves horizontally until they match with their neighbors, if the scale is fixed for a hypothetical curve at 204 °C. Since a curve does not exist for the desired temperature, we can interpolate between 208.6 °C and 199.4 °C. The resulting master curve is plotted in Fig. 2.23.

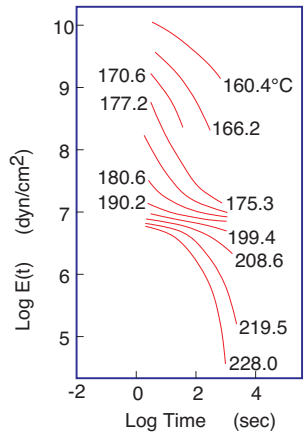

Figure 2.22 Stress relaxation data for poly-α-methylstyrene

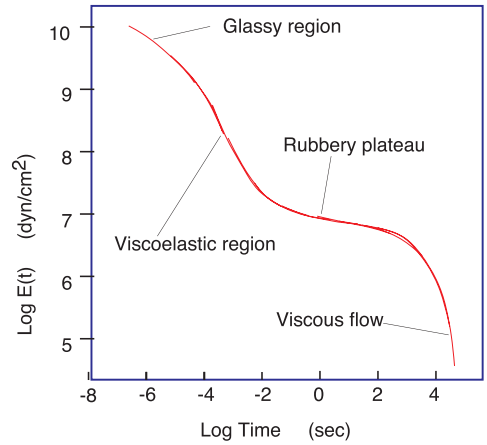

Figure 2.23 Master curve for poly-α-methylstyrene at 204 °C

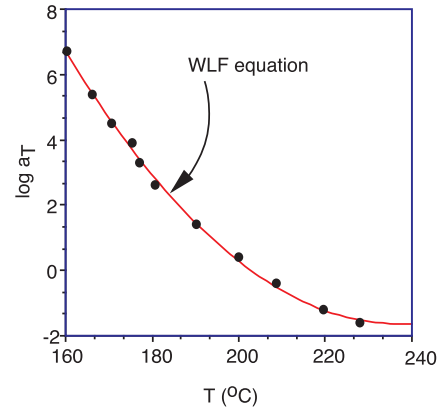

Figure 2.24 Shift factor and WLF for $T_{ref} = 204$ °C

The amount each curve must be shifted to meet the master curve is the shift factor, $\log a_T$. Figure 2.24 represents the shift factor versus temperature. The solid line indicates the shift factor predicted by the WLF equation. Good agreement can be seen.

Example 2.2 Creep-Isochronous Curves

In a special laboratory experiment, a PMMA pipe is used to cap a tank that is pressurized at 2 MPa, as shown in Fig. 2.25. The 3 mm thick pipe has a 50 mm internal diameter and

is 300 mm long. Estimate the diameter change of the pipe after one year of testing. Use the creep data given below (Fig. 2.26) [7].

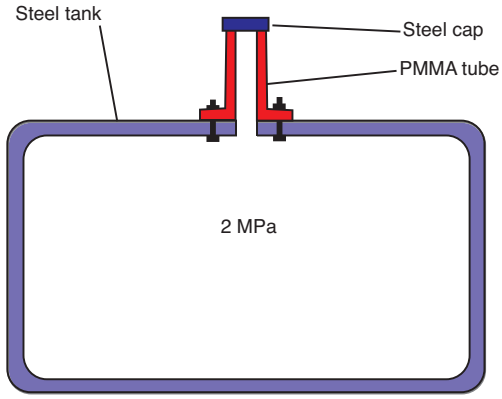

Figure 2.25 Schematic of the laboratory set-up

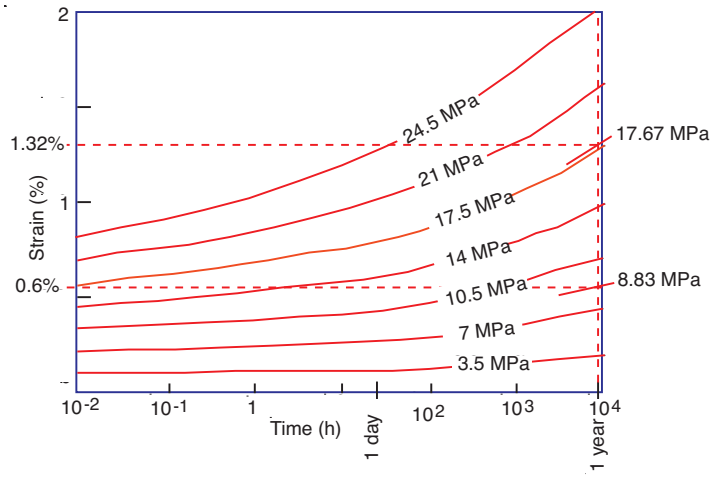

Figure 2.26 PMMA creep data

To solve this problem, we can use the thin pressure vessel approximation, working with an average diameter, $\overline{D} = 53$ mm. This is a case of biaxial stress, composed of a hoop stress, σ_H, and an axial stress, σ_A, defined by

$$\sigma_H = \frac{p\,\overline{D}}{2h} \quad \text{and} \quad \sigma_A = \frac{p\,\overline{D}}{4h}$$

where, p is the pressure and h is the thickness. These stresses are constant and will cause the pipe to creep. Using the PMMA creep data we can generate a 1-year isochronous curve, or we can determine the strains directly from the creep data. The strains corresponding to stresses of 17.67 MPa and 8.83 MPa are $\varepsilon_H = 1.32\,\%$ and $\varepsilon_A = 0.60\,\%$, respectively.

Since this is a biaxial case, we must correct the hoop strain using Poisson's effect, before computing the diameter change. For this we use

$$\varepsilon_{\mathrm{H}}^{\mathrm{corrected}} = \varepsilon_{\mathrm{H}} - \nu\varepsilon_{\mathrm{A}}$$

However, since we were not given Poisson's ratio, ν, we assume a value of ⅓. Thus,

$$\varepsilon_{\mathrm{H}}^{\mathrm{corrected}} = 1.38\,\% - (0.33)(0.6\,\%) = 1.12\,\%.$$

To compute the change in diameter we use

$$\varepsilon_{\mathrm{H}}^{\mathrm{corrected}} = \frac{\Delta D}{\overline{D}}$$

Hence,

$$\Delta D = (53\ \mathrm{mm})(0.0112) = 0.594\ \mathrm{mm}$$

Example 2.3 Creep — Isometric Curves

In the assembly shown in Fig. 2.27, a tubular polypropylene feature is pressed on a 15 mm long metal stud. The inner diameter of the 1 mm thick PP tubular element is 10 mm. The metal stud is slightly oversized with a diameter of 10.15 mm. With a coefficient of friction $\mu = 0.3$ estimate the force required to disassemble the parts shortly after assembly, and after one year. Use the creep data given in Fig. 2.8.

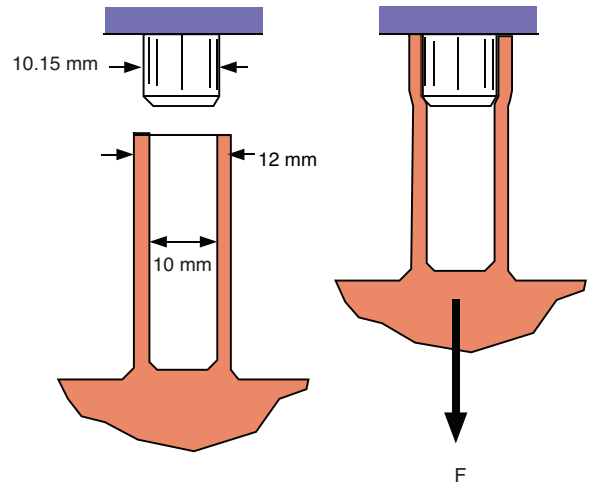

Figure 2.27 Press-fit assembly

This is a classic constant strain, ε_0, stress relaxation problem. The initial hoop stress that holds the assembly together can be quite high. However, as time passes, the hoop stress

relaxes and it becomes easier to disassemble the two components. The strain in the system after assembly is computed using

$$\varepsilon_0 = \frac{\Delta D}{\overline{D}} = \frac{0.15\,\text{mm}}{11.0\,\text{mm}} = 0.0145 \rightarrow 1.45\%$$

In order to follow the hoop stress history after assembly, we generate a 1.45 % isometric curve, which is shown in Fig. 2.28.

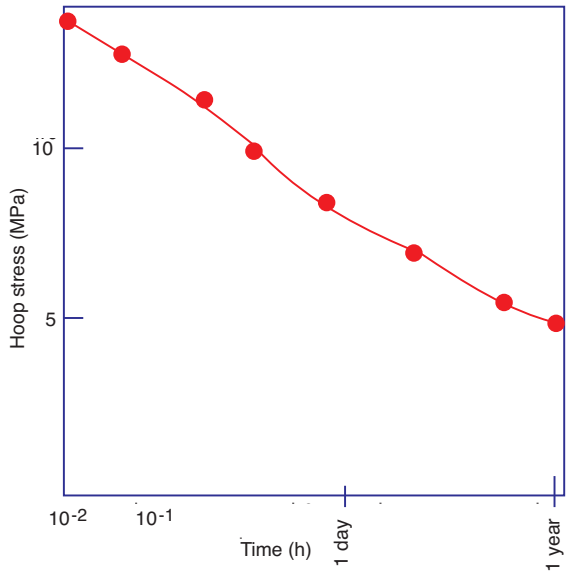

Figure 2.28 Isometric curve for a 1.45 % strain, derived from Fig. 2.8

From the isochronous curve we can deduce that the hoop stress, σ_H, is 13.7 MPa shortly after assembly and about 5 MPa one year after assembly. The pressure acting on the metal stud, due to the hoop stress, can be computed using

$$p = \frac{2h\,\sigma_H}{\overline{D}}$$

which gives a 2.49 MPa pressure right after assembly and 0.91 MPa after one year. From the pressure and the friction we can calculate the disassembly force with

$$F = \mu p(\pi DL)$$

where $L = 15$ mm is the length of the stud. Using the above equation, the computed force necessary to pull the two components apart is 358 N (80 lb) after assembly and 130 N (29 lb) after one year.

References

1. Castiff, E. and A.V.J. Tobolsky, *Colloid Sci.* (1955), *10*, 375

2. Williams, M.L., R.F. Landel, and J.D. Ferry, *J. Amer. Chem. Soc.* (1955), *77*, 3701
3. Osswald, T.A., E. Baur, S. Brinkmann and E. Schmachtemberg, *International Plastics Handbook*, Hanser Publishers (2006), Munich
4. Treloar, L.R.G., *The Physics of Rubber Elasticity*, 3rd Ed. (1975), Clarendon Press, Oxford
5. Courtesy ICIPC, Medellín, Colombia.

6. Guth, E., and R. Simha, *Kolloid-Zeitschrift* (1936), *74*, 266

6. Osswald, T.A., and G. Menges, *Materials Science of Polymers for Engineers*, Hanser Publishers (2003) Munich
7. Smallwood, H.M., *J. Appl. Phys.* (1944), *15*, 758
8. Mullins, L., and N.R. Tobin, *J. Appl. Polym. Sci.* (1965), *9*, 2993
9. ASTM, Plastics (II), 08.02, ASTM (1994), Philadelphia
10. Erhard, G., *Designing with Plastics*, Hanser Publishers (2006), Munich
11. Richard, K., E. Gaube and G. Diedrich, *Kunststoffe* (1959), *49*, 516
12. Gaube, E. and H.H. Kausch, *Kunststoffe* (1973), *63*, 391
13. Nielsen, L.E., and R.F. Landel, *Mechanical Properties of Polymers and Composites*, 2nd Ed., Marcel Dekker (1994), Inc., New York
14. Loos, R.D.A., *Processing of Composites*, Hanser Publishers (2000), Munich
15. Tsai, S.W., J.C. Halpin, and N.J. Pagano, *Composite Materials Workshop*, Technomic Publishing Co. (1968), Stamford
16. Brintrup, H., Ph.D. Thesis (1974), IKV, RWTH-Aachen, Germany
17. Menges, G., *Kunststoffverarbeitung III*, 5, Lecture notes (1987), IKV, RWTH-Aachen
18. Boyer, R.F., *Polymer Eng. Sci.* (1968), *8*, 161
19. Ehrenstein, G.W., *Polymeric Materials: Structure-Properties-Applications*, Hanser Publishers (2001), Munich
20. Menges, G., and H.-E. Boden, *Failure of Plastics*, Chapter 9, in W. Brostow, and R.D. Corneliussen (Eds.), Hanser Publishers (1986), Munich
21. Rest, H., Ph.D. Thesis (1984), IKV-Aachen
22. Erhard, G., *Designing with Plastics*, Hanser Publishers (2006), Munich
23. Riddell, M.N., *Plast. Eng.* (1974), *40*, 4, 71
24. Naranjo, A., M. Noriega, T. Osswald, A. Roldán and J.D. Sierra, *Plastics Testing and Characterization* (2008), Munich
25. Fujimoto, T., Ozaki, M. and Nagasawa, M., *J. Polymer Sci.* (1968), 2, 6, 129